Cell Death and Differentiation (2015) 22, 311–322

www.nature.com/cdd

Regulation of E2F1-induced apoptosis by poly(ADP-ribosyl)ation

A Kumari[1,2], T Iwasaki[1,3], S Pyndiah[2,4], EK Cassimere[2,5], CD Palani[1,6] and D Sakamuro*[,1,2]

The transcription factor adenovirus E2 promoter-binding factor (E2F)-1 normally enhances cell-cycle progression, but it also induces apoptosis under certain conditions, including DNA damage and serum deprivation. Although DNA damage facilitates the phosphorylation and stabilization of E2F1 to trigger apoptosis, how serum starvation renders cells vulnerable to E2F1-induced apoptosis remains unclear. Because poly(ADP-ribose) polymerase 1 (PARP1), a nuclear enzyme essential for genomic stability and chromatin remodeling, interacts directly with E2F1, we investigated the effects of PARP1 on E2F1-mediated functions in the presence and absence of serum. PARP1 attenuation, which increased E2F1 transactivation, induced G_2/M cell-cycle arrest under normal growth conditions, but enhanced E2F1-induced apoptosis in serum-starved cells. Interestingly, basal PARP1 activity was sufficient to modify E2F1 by poly(ADP-ribosyl)ation, which stabilized the interaction between E2F1 and the BIN1 tumor suppressor in the nucleus. Accordingly, BIN1 acted as an RB1-independent E2F1 corepressor. Because E2F1 directly activates the *BIN1* gene promoter, BIN1 curbed E2F1 activity through a negative-feedback mechanism. Conversely, when the BIN1–E2F1 interaction was abolished by PARP1 suppression, E2F1 continuously increased BIN1 levels. This is functionally germane, as PARP1-depletion-associated G_2/M arrest was reversed by the transfection of BIN1 siRNA. Moreover, PARP-inhibitor-associated anti-transformation activity was compromised by the coexpression of dominant-negative BIN1. Because serum starvation massively reduced the E2F1 poly(ADP-ribosyl)ation, we conclude that the release of BIN1 from hypo-poly(ADP-ribosyl)ated E2F1 is a mechanism by which serum starvation promotes E2F1-induced apoptosis.
Cell Death and Differentiation (2015) **22,** 311–322; doi:10.1038/cdd.2014.146; published online 26 September 2014

The growth of cancer cells may be attributable to an imbalance between cell proliferation and apoptosis, mediated by intrinsic signals (i.e., genetically programmed functions) and extrinsic stimuli (i.e., environmental stresses).[1,2] Therefore, if a cancer cell accumulates loss-of-function gene mutations in the cellular machinery essential for growth arrest or apoptosis, the cancer cell may become more malignant and display unlimited growth. The tumor-suppressor protein p53 is known to cause apoptosis under stress conditions, but an attempt to eradicate cancer cells by activating endogenous p53 may be unrealistic because the *TP53* gene is frequently mutated and dysfunctional in human malignancies.[3,4] Therefore, it is important to reactivate a proapoptotic protein whose gene is not often aberrantly expressed in cancer cells and whose function does not depend on p53. The transcription factor adenovirus E2 promoter-binding factor (E2F)-1, which is rarely mutated in cancer cells, can induce both p53-dependent and p53-independent apoptosis.[5–7] In response to DNA damage, E2F1 is phosphorylated and stabilized. E2F1 then activates a number of proapoptotic genes, including *APAF1*,[8,9] *caspase* genes,[10] *INK4A/ARF*,[11,12] *TP73*,[13] and *BIN1*.[14,15] Some of the encoded proteins, including BIN1, can induce apoptosis in the absence of p53.[14]

Like DNA damage, serum starvation sensitizes cells to E2F1-induced apoptosis.[5–7] For example, the overexpression of E2F1 induces apoptosis after serum deprivation *in vitro*.[5,6] Similarly, spontaneous tumors occur during tissue development in *E2f1*-knockout mice.[16,17] Given that 'micro-environmental' serum starvation occurs during dynamic tissue development, it is likely that aberrant cellular responses to 'micro-environmental' serum starvation arising from the loss of E2F1, such as disrupted E2F1-induced apoptosis, may trigger spontaneous cellular transformation *in vivo*. Although the RB1 tumor suppressor, an authentic E2F1 corepressor, induces G_1 arrest in the cell cycle,[18] most human malignancies are functionally defective in the RB1-associated pathway.

[1]Department of Biochemistry and Molecular Biology, Medical College of Georgia, Georgia Regents University Cancer Center, Augusta, GA 30912, USA; [2]Molecular Signaling Program, Stanley S. Scott Cancer Center, Louisiana State University Health Sciences Center, New Orleans, LA 70112, USA and [3]Laboratory of Molecular Biology, Research Center for Environmental Genomics, Kobe University, Kobe 657, Japan

*Corresponding author: D Sakamuro, Department of Biochemistry and Molecular Biology, Georgia Regents University Cancer Center, 1410 Laney Walker Blvd., Augusta, GA 30912, USA. Tel: +1 706 721 1018; Fax: +1 706 721 6608; E-mail: dsakamuro@gru.edu

[4]Current address: Institut de Génétique Moléculaire, Cibles Thérapeutiques, INSERM U940, Paris, France.

[5]Current address: Department of Biology, Texas Southern University, Houston, Texas 77004, USA.

[6]Current address: Department of Oral Health and Diagnostic Sciences, College of Dental Medicine, Georgia Regents University, Augusta, Georgia 30912, USA.

Abbreviations: E2F, adenovirus E2 promoter-binding factor; PARP1, poly(adenosine diphosphate [ADP]-ribose) polymerase 1; PAR, poly(ADP-ribose) polymer chain; BIN1, bridging integrator 1; BAR, BIN-Amphiphysin-Rvs homology domain; MBD, MYC-binding domain; SH3, src homology domain 3; MB, marked box domain; TA, transactivation domain; ER, estrogen receptor; GST, glutathione-*S*-transferase; HA, hemagglutinin; DAPI, 4′,6-diamidino-2-phenylindole; 4-OHT, 4-hydroxy tamoxifen; sh-/si-RNA, short hairpin-/small interfering-RNA; ChIP, chromatin immunoprecipitation; Luc, luciferase-reporter vector; qRT-PCR, quantitative reverse transcriptase-polymerase chain reaction; MEFs, mouse embryonic fibroblasts

Received 19.5.14; revised 16.8.14; accepted 18.8.14; Edited by RA Knight; published online 26.9.14

Because the loss of RB1 causes subsequent hyperactivation (or deregulation) of E2F1, which should theoretically activate both cell-cycle progression and apoptosis,[19] we hypothesized that cancer cells constitutively expressing deregulated E2F1 must have an RB1-independent mechanism that does not allow E2F1 to induce apoptosis during serum starvation, but that instead leaves E2F1-induced cell-cycle progression intact.

Poly(adenosine diphosphate [ADP]-ribose) polymerase 1 (PARP1; EC 2.4.2.30) is a nuclear enzyme that acts as a molecular sensor, detecting single-stranded DNA lesions.[20,21] The enzyme also promotes the deconcentration of higher-order chromatin structures by modifying histone poly(ADP-ribosyl)ation. Consequently, PARP1 acts as a regulatory component of multiprotein transcriptional complexes on the chromatin.[21,22] Because PARP1 is abundant in cancer cells,[23] PARP1 inhibition might counterbalance the oncogenic potential of cancer cells by reprogramming the transcriptional profiles of PARP1-modified genes. Consistent with this premise, PARP1 physically interacts with several cancer-related transcription factors, including E2F1.[24]

In this paper, we report that under optimized growth conditions, the basal activity of PARP1 naturally poly(ADP-ribosyl)ates E2F1 and stabilizes the interaction between E2F1 and the BIN1 tumor suppressor in the nucleus. BIN1 thus represses E2F1 activity regardless of RB1. In contrast, when PARP1 is deficient, hypo-poly(ADP-ribosyl)ated E2F1 releases proapoptotic BIN1, thereby rendering cells more susceptible to serum-starvation-induced apoptosis. Because serum starvation greatly reduces E2F1 poly(ADP-ribosyl) ation, we propose a previously uncharacterized regulatory mechanism for E2F1-induced apoptosis during serum starvation, which correlates inversely with E2F1 poly(ADP-ribosyl) ation and the E2F1–BIN1 interaction.

Results

Basal PARP1 activity is essential to restrain endogenous E2F1 activity. The transcription factor E2F1 promotes cell-cycle progression, but it also induces apoptosis during serum starvation.[5–7] Because PARP1 regulates gene transcription[21,22] and interacts directly with E2F1,[24] we tested whether PARP1 alters E2F1-dependent transcription. As the PARP1-deficient cell system, we used the *Parp*$^{-/-}$ 3T3 fibroblast line, together with its parental control line, the *Parp*$^{+/+}$ 3T3 fibroblast cell line.[25] To avoid any interference (or synergistic effect) by endogenous RB1, we used two RB1-deficient human cancer cell lines, DU145 (prostate cancer) and SAOS2 (osteosarcoma), in which endogenous PARP1 was depleted by the stable infection of recombinant lentiviruses expressing short-hairpin RNA directed against PARP1 (sh-PARP1). A scrambled sh-RNA-expressing lentivirus was used as the negative control (sh-control).

The transcriptional activity of endogenous E2F1 was monitored by transfection of the adenovirus *E2A* gene promoter-driven luciferase vector (E2A–Luc), an E2F-sensitive promoter-driven reporter vector.[14,15,26] In the *Parp1*$^{-/-}$ 3T3 fibroblast line, endogenous E2f1 levels were not altered, but its transcriptional activity was significantly increased (Figure 1a). Similarly, in the RB1-deficient cancer lines, PARP1 depletion increased endogenous E2F activity, which was clearly suppressed by co-transfected *RB1* (Figure 1b), implying that PARP1 was dispensable for RB1-dependent E2F repression and *vice versa*. Furthermore, the small-molecule PARP inhibitors, olaparib and PJ-34, which almost completely abolished cellular poly(ADP-ribosyl)ation, increased E2A–Luc activity (Figure 1c).

Among the E2F family of transcription factors, only E2F1, E2F2, and E2F3a act as transcriptional activators and can be suppressed by RB1.[18] Interestingly, in DU145 and SAOS2 lines, the sh-PARP1-induced E2A–Luc activity was suppressed only when small-interfering RNA (siRNA) directed against E2F1, but not siRNA for E2F2 or E2F3, was co-transfected (Figure 1d). These results suggest that the basal catalytic activity of PARP1 is essential for specifically suppressing endogenous E2F1 activity in a manner independent of (or parallel to) the RB1-dependent E2F1 repression.

PARP1 depletion promotes E2F1-dependent apoptosis, but retards the cell cycle. Consistent with the fact that PARP1 inactivation enhanced E2F1 activity (see above, Figure 1), a qRT-PCR analysis showed that the expression of E2F1 transcriptional targets related to cell-cycle progression, such as Cyclin E and Cyclin B, was upregulated in PARP1-deficient DU145 cells (Figure 2a). However, treatments with olaparib significantly reduced the growth rates of the DU145 cells (Figure 2b), which was accompanied by G_2/M cell-cycle arrest (Figure 2c). Similarly, decreased PARP1 was sufficient to induce G_2/M arrest under optimal growth conditions in DU145 cells (Supplementary Figure 1). Interestingly, olaparib did not reduce the already slow growth rate of *Parp1*$^{-/-}$ 3T3 fibroblasts, but meaningfully suppressed the proliferation of *Parp1*$^{+/+}$ 3T3 fibroblasts (Supplementary Figure 2a). Consistently, the same PARP inhibitor failed to induce G_2/M arrest in *Parp1*$^{-/-}$ 3T3 fibroblasts (Supplementary Figure 2b). We concluded that the basal activity of PARP1 is essential for G_2/M cell-cycle transition in both normal and cancer cells.

To examine a direct role of PARP inhibition in E2F1-induced cell-cycle progression, we constitutively expressed a full-length E2F1 protein fused to the recombinant estrogen receptor (ER) (ER-E2F1) in *E2f1*-knockout mouse embryonic fibroblasts (MEFs/*E2f1*$^{-/-}$).[14] The estrogen derivative, 4-hydroxy tamoxifen (4-OHT), stimulates the migration of the cytoplasmic ER fusion protein into the nucleus. Therefore, the ER-E2F1 fusion protein acts as a functional E2F1 transcription factor. ER-E2F1 activity was monitored with a transfected E2A–Luc reporter gene. We observed that the E2A–Luc activity in the presence of 4-OHT was further increased by olaparib (Figure 2d), but that, concomitantly, ER-E2F1-dependent cell proliferation was inhibited by the same PARP inhibitor (Figure 2e). As predicted, olaparib-induced growth suppression was associated with G_2/M cell-cycle arrest (Figure 2f). Using the same E2F1-inducible cell system, we also found that E2F1-dependent apoptosis during serum deprivation was promoted further by PARP inhibition (Figure 2g). These results suggest that impaired PARP1-induced E2F1 activity sensitizes cells to E2F1-induced apoptosis, but does not allow E2F1 to promote the cell cycle (Figure 2h).

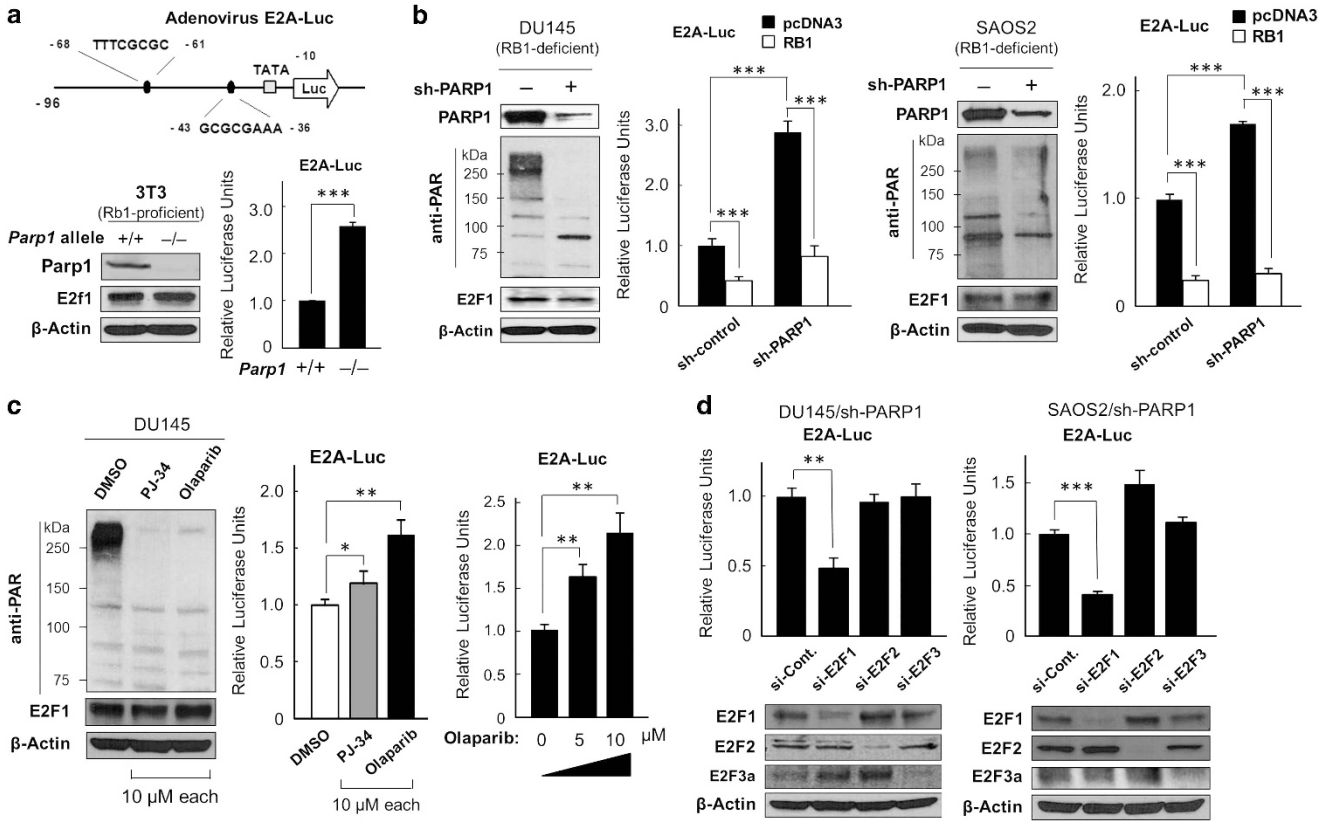

Figure 1 PARP1 is essential for repressing E2F1-induced transcription, regardless of RB1. (**a**) Endogenous E2F activity was monitored by the transfection of mouse 3T3 *Parp1*$^{+/+}$ and *Parp1*$^{-/-}$ fibroblasts with E2A–Luc, an adenoviral *E2A*-promoter-driven luciferase reporter vector.[14,15] The *E2A* gene promoter contains a TATA box, followed by two canonical E2F-consensus sequences: 5′-GCGCGAAA-3′ and 5′-TTTCGCGC-3′.[26] Parp1 and E2f1 levels were determined with western blotting. β-Actin was used as the internal loading control. ***$P<0.0005$. (**b**) Two RB1-defective human cancer cell lines, DU145 and SAOS2, were stably infected with a short hairpin (sh)-PARP1 recombinant lentivirus and subjected to western analysis, with an anti-poly(ADP-ribose) polymer chain antibody (anti-PAR). The effects of sh-PARP1 and RB1 transfection on endogenous E2F activity were monitored with E2A–Luc assays. ***$P<0.0005$. (**c**) DU145 cells were treated with PJ-34 or olaparib for 72 h and subjected to western analysis with an anti-PAR antibody or E2A–Luc assay. *$P<0.05$, **$P<0.005$. (**d**) DU145/sh-PARP1 and SAOS2/sh-PARP1 cell lines were cotransfected with siRNA directed against E2F1, E2F2, or E2F3a and E2A–Luc. The depletion of each E2F protein was checked with a western analysis. si-Control RNA (si-Cont.) was used as the negative control. **$P<0.005$

PARP1 post-translationally modifies E2F1 by poly(ADP-ribosyl)ation. PARP1 post-translationally modifies histones H1 by poly(ADP-ribosyl)ation and modulates gene transcription.[20–22] However, the inhibition of basal PARP1 activity was sufficient to increase endogenous E2F1 activity monitored by transiently transfected E2A–Luc vector (see Figure 1). Therefore, we assumed that PARP1 might naturally poly(ADP-ribosyl)ate a non-histone protein on a naked E2F-sensitive gene promoter to inhibit its promoter activity. Because PARP1 physically associates with E2F1,[24] we tested whether PARP1 modifies E2F1 by poly(ADP-ribosyl)ation.

The immunoprecipitation (IP) of endogenous E2F1, followed by western blot analysis with an anti-poly(ADP-ribose) polymer chain (anti-PAR) antibody, revealed that, under normal optimized conditions, E2F1 was poly(ADP-ribosyl) ated, only in the presence of PARP1 (Figure 3a). Consistently, hydrogen peroxide (H_2O_2), which robustly stimulates endogenous PARP1 activity, enhanced E2F1 poly(ADP-ribosyl) ation (Figure 3b). Because a brief treatment with H_2O_2 concurrently suppressed endogenous E2F1 activity (Figure 3c), we assumed that, when poly(ADP-ribosyl)ated, the stability of endogenous E2F1 protein on an E2F-sensitive gene promoter might be reduced. However, chromatin immunoprecipitation (ChIP) assays revealed that treatments with H_2O_2 even increased the levels of E2F1 protein bound to the *E2A* promoter (Figure 3d), implying that a transcriptionally negative function might be recruited by poly(ADP-ribosyl) ated E2F1.

As increased E2F1 activity is essential for E2F1-induced apoptosis,[5–7] we wondered whether the levels of E2F1 poly (ADP-ribosyl)ation might be diminished after serum starvation. Consistent with this theory, we observed that, in 3T3 *Parp1*$^{+/+}$ fibroblast cells, E2f1 poly(ADP-ribosyl)ation was considerably reduced during serum starvation (Figure 3e). Concurrently, the endogenous Parp1 levels and the entire cellular poly(ADP-ribosyl)ation were diminished (Figure 3f). This is probably attributable to the lack of endogenous c-Myc after serum withdrawal in untransformed cells, as PARP1 expression and activity are activated by c-MYC.[27,28] These results suggest that PARP1 post-translationally modifies E2F1 by poly(ADP-ribosyl)ation, which subsequently stabilizes the E2F1–DNA promoter interaction, and negatively regulates E2F1-dependent gene transcription.

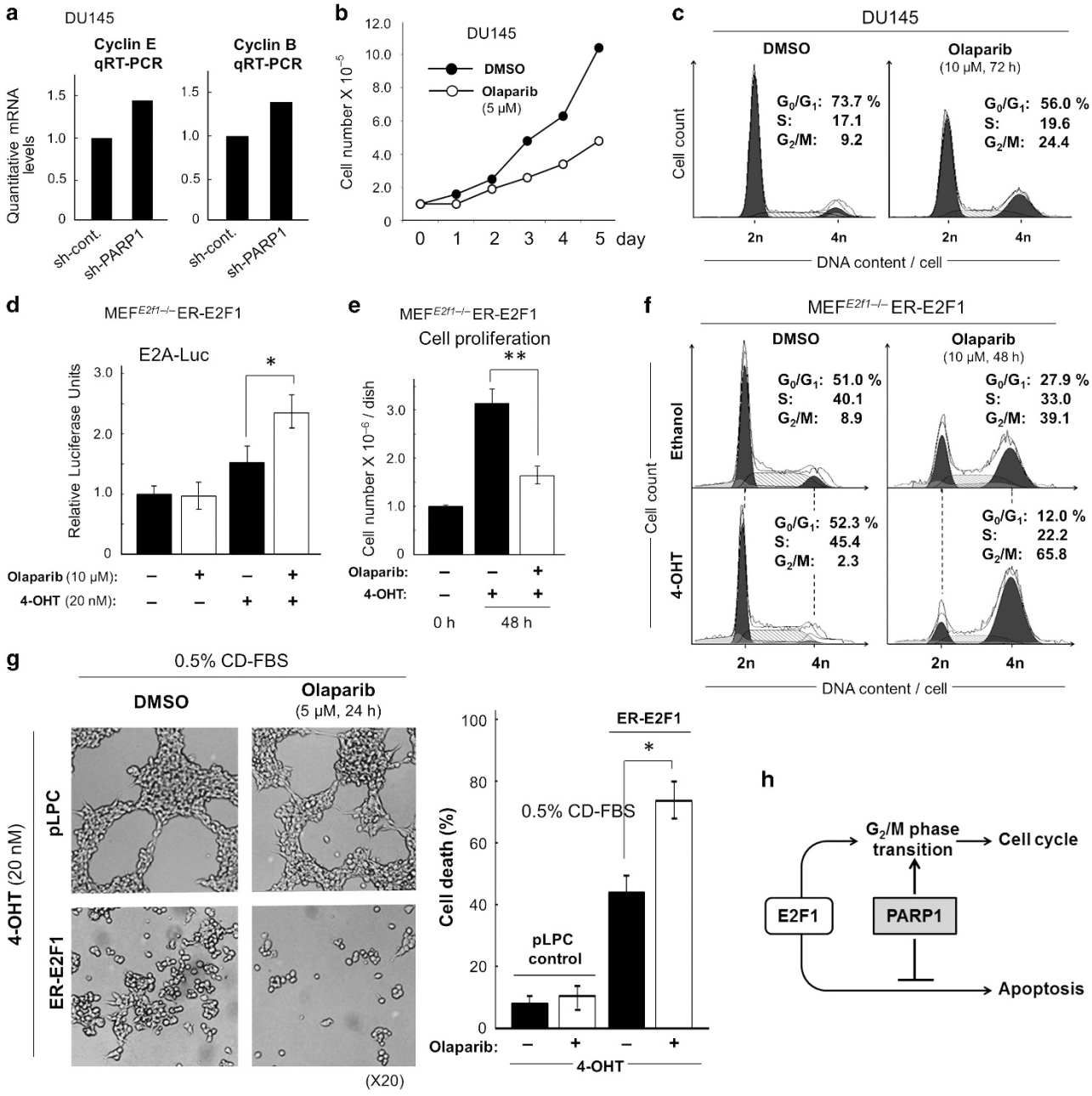

Figure 2 PARP inhibition retards E2F1-induced cell-cycle progression, but stimulates E2F1-induced apoptosis during serum starvation. (**a**) Quantitative real-time RT-PCR (qRT-PCR) analysis of endogenous cyclin E and cyclin B mRNAs expressed in DU145 ± sh-PARP1 cells. Endogenous glyceraldehyde 3-phosphate dehydrogenase (GAPDH) mRNA was used as the internal control. (**b**) Growth curve analysis of DU145 cells treated with or without olaparib (5 μM). (**c** and **f**) Flow cytometric analyses. Indicated cell lines were cultured with or without olaparib (10 μM), collected by trypsinization, stained with propidium iodide, and subjected to cell-cycle analyses. (**d**) E2A–Luc reporter assays in *E2f1*$^{-/-}$ mouse-embryo fibroblasts (MEFs) constitutively expressing the ER-E2F1 fusion protein (MEF$^{E2f1-/-}$ER-E2F1), which were cultured for 48 h in growth medium (supplemented with 10% Charcoal/Dextran (CD)-treated fetal bovine serum (FBS)) in the presence (+) or absence (–) of olaparib (10 μM) and 4-OHT (20 nM). *$P<0.05$. (**e**) The adherent (i.e., proliferating) cells (cultured in 10% CD-FBS–containing growth medium) and (**g**) the floating (dead) cells (cultured in 0.5% CD-FBS plus 4-OHT–containing medium) were subjected to trypan-blue staining for counting. *$P<0.05$, **$P<0.005$. (**h**) In the absence of PARP1, E2F1-dependent transcription is upregulated (see Figure 1), which is, however, insufficient to properly promote the cell cycle mediated by E2F1, because of the lack of PARP1-dependent G_2/M phase transition. In contrast, E2F1-dependent apoptosis during serum starvation is accelerated further in PARP1-deficient cells

BIN1 is a PARP1-interacting E2F1 corepressor independent of RB1. Because PARP1 *per se* has no structural features characteristic of a transcriptional corepressor,[20,21] we hypothesized that PARP1 recruits a corepressor to the vicinity of E2F1. Among a number of PARP1-interacting proteins in the nucleus, the bridging integrator 1 (BIN1) protein,[27] which was originally identified as a MYC-interacting proapoptotic tumor suppressor,[29] acts as a broad transcriptional corepressor.[30] Co-immunoprecipitation (co-IP) experiments followed by western blot analysis revealed that BIN1

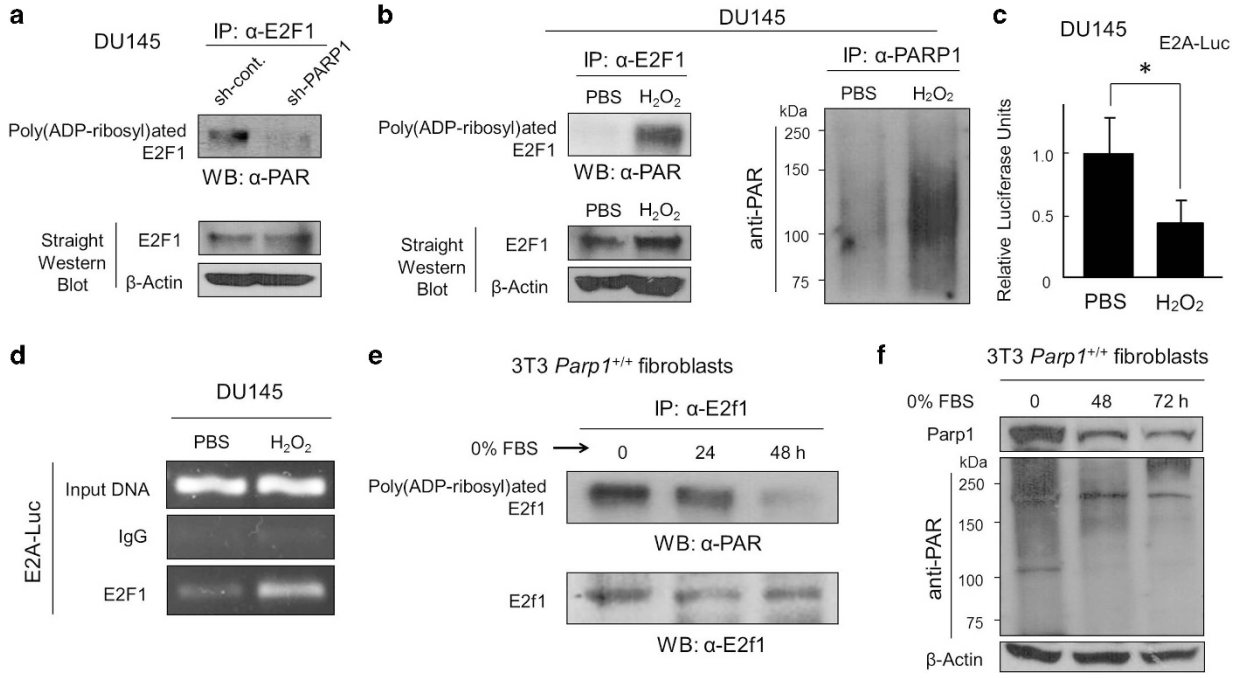

Figure 3 PARP1 modifies E2F1 by poly(ADP-ribosyl)ation. (**a**) IP/Western analysis of poly(ADP-ribosyl)ated E2F1 in DU145 ± sh-PARP1 cells. (**b**) IP/western analysis of poly(ADP-ribosyl)ated E2F1 in DU145 cells cultured with or without H_2O_2 (10 μM) for 30 min. (**c**) E2A–Luc assays in DU145 cells with or without H_2O_2 (10 μM) for 30 min. *$P<0.05$. (**d**) ChIP analysis of endogenous E2F1 protein on E2A–Luc promoter with or without H_2O_2 (10 μM) for 30 min. (**e**, **f**) The mouse 3T3 *Parp1*$^{+/+}$ fibroblasts were incubated in culture medium containing 0% FBS for the times indicated. Pre-cleared protein lysates were subjected to either IP with an anti-E2f1 antibody followed by western analysis with an anti-PAR antibody or directly to western analysis with an anti-E2f1 antibody, an anti-Parp1 antibody, or an anti-PAR antibody

interacted physically with E2F1 *in vivo*, regardless of the status of the *RB1* gene (Figure 4a).

Domain-mapping experiments established that the BIN1 coiled-coil BIN-Amphiphysin-Rvs (BAR) homology domain, which is necessary and sufficient for BIN1-mediated growth suppression,[31] was required for the E2F1–BIN1 interaction *in vitro* (Figure 4b). In contrast, the E2F1 marked box (MB) domain, which was not essential for its interaction with RB1, was necessary for BIN1 binding (Figure 4c). However, the E2F1 C-terminal transactivation (TA) domain, which is known to be sufficient to support the E2F1-RB1 interaction,[18] did not participate in the BIN1–E2F1 interaction (Figure 4c). The BIN1–E2F1 interaction is functionally relevant, as heterologously expressed BIN1 suppressed endogenous E2F1 activity, even in RB1-deficient cells (Figure 4d). Conversely, depletion of endogenous BIN1 was sufficient to release endogenous E2F1 activity in two RB1-deficient lines, SAOS2 (Figure 4e) and DU145, and three RB1-proficient lines, SK-MEL-28 (human melanoma), LNCaP (prostate cancer), and WI38 (human diploid fibroblast) (Supplementary Figure 3). These results suggest that, in optimal culture conditions, BIN1 interacts with E2F1 and represses its transactivation regardless of the RB1-dependent repression of E2F1.

PARP1 facilitates the E2F1–BIN1 interaction in the nucleus. We have previously reported that the BIN1 BAR-C domain (the carboxyl-terminal half of the BAR domain) is sufficient to interact with PARP1.[27] Because the same BIN1 BAR-C domain was required for BIN1–E2F1 binding (see above; Figure 4b), we wondered whether PARP1 might disrupt the BIN1–E2F1 interaction. However, a co-IP/western blot analysis demonstrated that the BIN1–E2F1 association *in vivo* was even stabilized in the presence of PARP1 (Figure 5a). Similarly, heterologously expressed BIN1 remarkably stabilized endogenous E2F1–PARP1 interaction (Figure 5b), implying that PARP1 and BIN1 mutually assist their interaction with E2F1. Consistent with this premise, ChIP assays revealed that the amount of endogenous BIN1 protein on the *E2A* promoter was significantly reduced in *Parp1*$^{-/-}$mouse fibroblasts (Figure 5c). Furthermore, in Parp1-deficient cells, exogenously expressed BIN1 failed to repress E2A–Luc activity, whereas transfected *RB1* suppressed it (Figure 5d), suggesting that the BIN1–E2F1 interaction, but not the RB1–E2F1 interaction, largely depends on endogenous PARP1.

Treatments with H_2O_2 reduced endogenous E2F1 activity (see Figure 3c). In parallel, BIN1 interacted with E2F1 and repressed its transcription (see Figure 4). Therefore, we hypothesized that E2F1 has a greater BIN1-binding affinity when it is poly(ADP-ribosyl)ated. In two independent cell lines, DU145 (RB1-deficient) and SK-MEI-28 (RB1-proficient), a brief treatment with H_2O_2 did not alter the levels of endogenous BIN1 and E2F1 (data not shown), but the BIN1–E2F1 interaction was markedly stabilized when cells were treated with H_2O_2 (Figure 5e). Moreover, *in situ* immunofluorescence microscopic analysis revealed that the nuclear localization of endogenous BIN1 protein was disturbed when PARP1 was depleted or inactivated (Figure 5f). These results suggest that PARP1 activity does not merely secure BIN1–E2F1 binding in the nucleus, but also allows

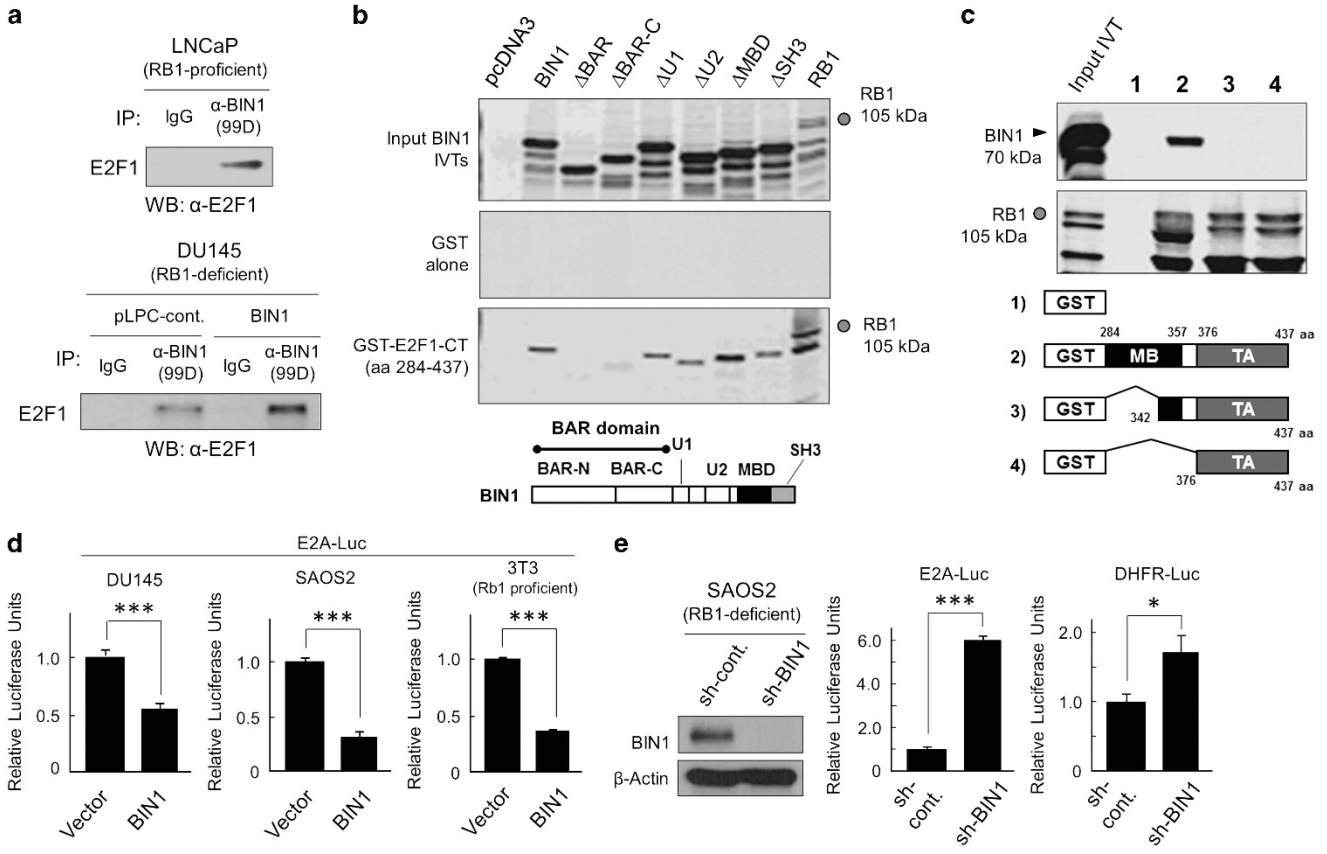

Figure 4 BIN1 interacts with E2F1 and inhibits its transactivation regardless of RB1. (**a**) Western blot analysis of endogenous E2F1 protein co-immunoprecipitated (co-IPed) with BIN1. The 99D anti-BIN1 monoclonal antibody, which recognizes the exon 13-encoding region corresponding to the part of the BIN1 MYC-binding domain (MBD),[30,54] was used for the co-IP experiments. (**b**, **c**) Glutathione-*S*-transferase (GST)-E2F1 fusion protein pull-down assays. [^{35}S]-methionine/cysteine-labeled *in vitro* transcription/translation products (IVTs) of BIN1 (70 kDa) or its deletion mutants were incubated with GST alone or GST-E2F1-CT (CT: carboxy-terminal half, amino acid (aa) 284–437) (or its deletion mutants) at 4 °C for 2 h. Co-precipitated radioactive materials were subjected to SDS-PAGE and fluorographed. [^{35}S]-labeled IVT of RB1 (105 kDa) was used as the positive control for E2F1 binding. BAR: BIN1-Amphiphysin-Rvs-homology domain; U1/2: regions unique to BIN1; MBD: MYC-binding domain; SH3: Src homology domain 3; MB: marked box domain; TA: transactivation domain. (**d**) CMV-BIN1 or (**e**) sh-BIN1 expression vector DNA was transiently transfected in the cell lines indicated for 48 h. Endogenous E2F activity was monitored by co-transfection of E2A–Luc or DHFR–Luc reporter vector. DHFR: dihydrofolate reductase. $^{*}P<0.05$, $^{***}P<0.0005$

BIN1 to localize to the nucleus. We concluded that basal PARP1 activity post-translationally modifies E2F1 by poly (ADP-ribosyl)ation, which stabilizes the BIN1–E2F1 interaction in the nucleus, thereby repressing the transcription of E2F1-responsive genes irrespective of RB1 levels.

PARP1 depletion cancels the E2F1 negative-feedback loop and robustly increases BIN1 levels. We reported previously that the activity of the *BIN1* gene promoter is directly upregulated by E2F1, particularly when RB1 is deficient.[14] In this study, we found that BIN1 physically interacted with E2F1 and repressed its transactivation in a manner independent of RB1 (see Figure 4), but dependent on PARP1 (see Figure 5). Therefore, we propose an E2F1 negative-feedback loop mechanism that is dependent on intact PARP1. If this is the case, inhibition of PARP1 should abolish the negative-feedback loop, thereby facilitating the dissociation of BIN1 (an E2F1 corepressor) from E2F1. Accordingly, endogenous E2F1 may robustly activate a number of E2F1-target transcriptions, including *BIN1*, but, this time, BIN1 should not interact with and repress E2F1, as E2F1 is hypo-poly(ADP-ribosyl)ated.

To validate this model, we first performed ChIP assays to detect an endogenous BIN1 protein on the human *BIN1* gene promoter, which contains active E2F-consensus sites.[14] We found that, when PARP1 was inactivated, the levels of endogenous BIN1 protein on the *BIN1* promoter DNA were considerably attenuated (Figure 6a). This result was also supported by the cytoplasmic localization of endogenous BIN1 after PARP1 attenuation (see Figure 5f) and demonstrated that the BIN1-dependent E2F1 repression was canceled when PARP1 was deficient. As predicted, PARP1 depletion (Figure 6b) or PARP inhibition (Figure 6c) consistently increased endogenous BIN1 levels by activating the *BIN1* gene promoter. Furthermore, the induction of mouse *Bin1* mRNA by the treatment with olaparib was reversed by the co-transfection of E2f1 siRNA, as was the induction of the regular proapoptotic target gene of E2f1, *Apaf1* (Figure 6d).

PARP2, like PARP1, catalyzes the poly(ADP-ribosyl)ation of several nuclear proteins with nicotinamide adenine dinucleotide (NAD^+) as a substrate.[32,33] Although the majority of

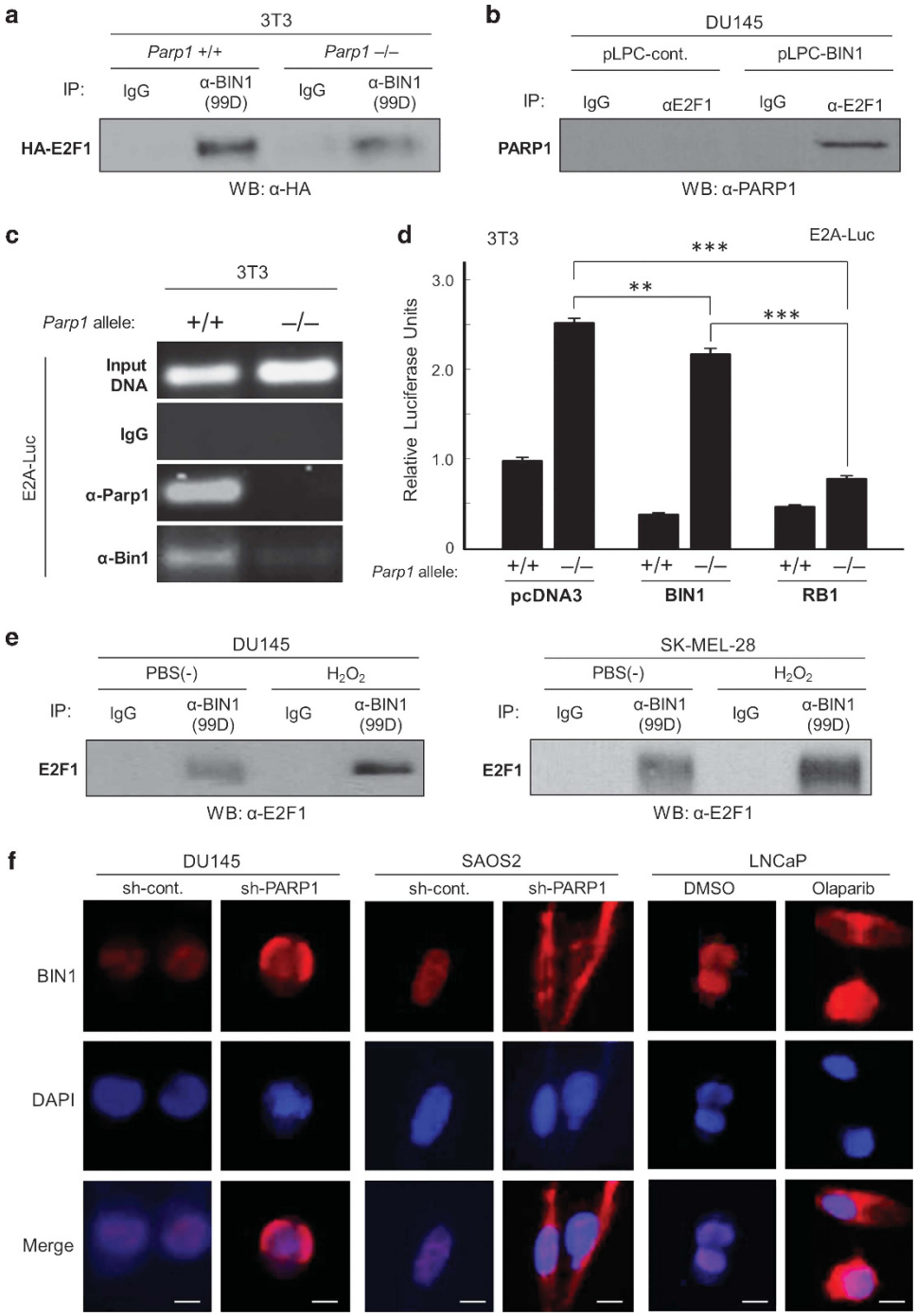

Figure 5 PARP1 stabilizes the E2F1–BIN1 interaction in the nucleus. (**a**) Western blotting analysis of HA-tagged E2F1 protein (HA–E2F1) co-immunoprecipitated (co-IPed) with exogenously co-expressed BIN1 in the presence or absence of Parp1 in mouse 3T3 fibroblasts. (**b**) Western analysis of endogenous PARP1 protein co-IPed with endogenous E2F1 in the presence or absence of overexpressed BIN1 in DU145 cells. (**c**) Chromatin immunoprecipitation (ChIP) assay in mouse 3T3 *Parp1*$^{+/+}$ and *Parp1*$^{-/-}$ fibroblast lines transiently transfected with E2A–Luc. Endogenous mouse Parp1 and Bin1 proteins were co-IPed with the *E2A* promoter. (**d**) E2A–Luc reporter assays in 3T3 *Parp1*$^{+/+}$ and *Parp1*$^{-/-}$ fibroblast cells cotransfected with pcDNA3, *BIN1*, or *RB1*. ***$P < 0.0005$. (**e**) Western blot analysis of endogenous E2F1 protein co-IPed with an anti-BIN1 (clone 99D) antibody after treatment with or without H_2O_2 (10 μM, 30 min) in two independent cell lines, DU145 (RB1-deficient) and SK-MEL-28 (RB1-proficient). (**f**) *In situ* immunofluorescence microscopy. Subcellular localization of endogenous BIN1 protein (red) was detected with an anti-BIN1 antibody (clone D3). DAPI was used for nuclear counterstaining (blue). Scale bar = 10 μM

cellular poly(ADP-ribosyl)ation is attributed to PARP1, PARP2 may act as an alternative enzyme, particularly when PARP1 is unavailable.[32,33] Similar to other small-molecule PARP inhibitors, olaparib inhibits not only PARP1 but also PARP2.[34] Nonetheless, olaparib did not induce the expression of endogenous Bin1 transcripts in 3T3 *Parp1*$^{-/-}$ fibroblasts (Figure 6e), suggesting that inhibition of PARP1, but not PARP2, is essential for releasing endogenous E2F1 activity.

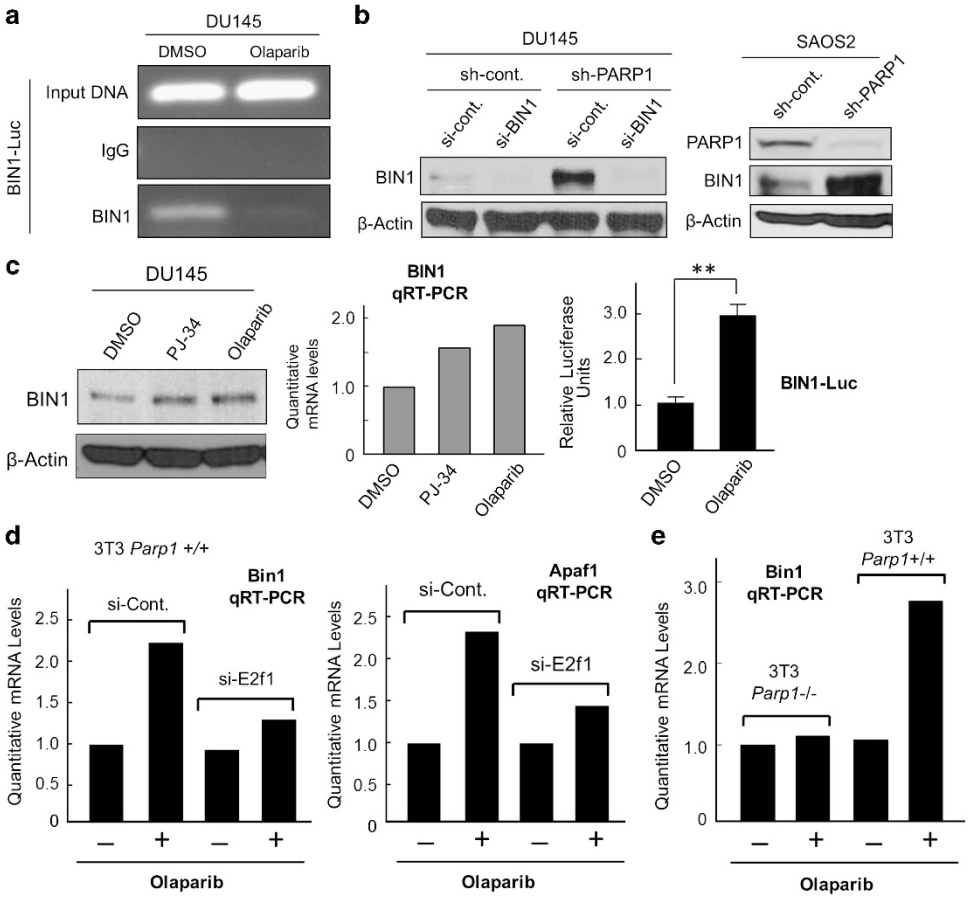

Figure 6 PARP1 attenuation abolishes the E2F1 negative-feedback loop and robustly increases BIN1 levels. (**a**) Endogenous BIN1 levels on the BIN1–Luc promoter were analyzed by chromatin immunoprecipitation (ChIP) assays in DU145 cells pretreated with DMSO or olaparib (10 μM, 72 h). (**b**, **c**) PARP1 depletion by sh-PARP1 or PARP1 inhibition by PJ-34 (10 μM, 72 h) or olaparib (10 μM, 72 h) was sufficient to increase BIN1 proteins, BIN1 transcripts, and *BIN1* promoter activity in human cancer cells. $^{**}P < 0.005$. (**d**) qRT-PCR analyses of Bin1 and Apaf1 mRNA expression in mouse 3T3 *Parp1*$^{+/+}$ fibroblasts transiently transfected with E2f1 si-RNA (si-E2f1), followed by the treatments with (+) or without (–) olaparib (10 μM, 72 h). As the negative control, scrambled si-control RNAs (si-Cont.) were used. (**e**) qRT-PCR analysis of Bin1 mRNA expression in mouse 3T3 *Parp1*$^{+/+}$ and *Parp1*$^{-/-}$ cells treated with (+) or without (–) olaparib (10 μM, 72 h)

Together, we concluded that PARP1 deficiency, which destabilizes the E2F1–BIN1 interaction (see Figure 5a), disturbs the E2F1 negative-feedback loop, thereby robustly stimulating endogenous *BIN1* expression.

BIN1 is required for the anti-oncogenic functions mediated by PARP1 inhibition. It is well known that BIN1 suppresses oncogenic transformation[29,30] by stimulating apoptotic cell death[14,27,35,36] and/or arresting the cell cycle.[15,27,31] To determine whether the induction of endogenous BIN1 mediated by PARP1 attenuation is biologically germane, we performed several cell-based assays. First, three different pharmacological PARP inhibitors, niraparib, olaparib, and veliparib, demonstrate different cytotoxic and cytostatic effects in cancer cells,[34] so we hypothesized that a more powerful PARP inhibitor should induce more BIN1 expression. Consistent with this theory, we observed that, in *Parp1*$^{+/+}$ 3T3 fibroblasts, the cytotoxic and/or cytostatic effects of these PARP inhibitors were correlated with their capacities to induce endogenous *Bin1* expression (Figure 7a). Second, transient transfection of Bin1 siRNA significantly reduced both the olaparib-induced G_2/M arrest in 3T3 *Parp1*$^{+/+}$ cells (Figure 7b) and the sh-PARP1–associated G_2/M arrest in DU145 cells (Supplementary Figure S4). Third, olaparib massively suppressed oncogenic Ras/HPV16 E7 cotransformation, which was reversed when BINΔ4, a BIN1 dominant-negative inhibitor,[35] was co-transfected (Figure 7c). BINΔ4 lacks only a 6-amino-acid sequence, KLVDVD, within the BIN1 coiled-coil BAR effector domain[31,37] and thus compromises the proapoptotic BIN1 function.[35] Computer-based prediction of the three-dimensional structure of a BIN1 BAR domain-alone peptide using the SWISS-MODEL server[38] and the Phyre server[39] demonstrated that the KLVDVD deletion slightly abolished a proper effector structure of the BIN1 coiled-coil BAR domain with minimum impacts on its flanking domains (or regions) of BIN1 (Supplementary Figure 5). Because serum starvation markedly reduced not only the E2F1 poly(ADP-ribosyl)ation, but also the entire PARP1 levels (see Figures 3e and f), these results suggest that the release of BIN1 from hypo-poly(ADP-ribosyl)ated E2F1 is a mechanism by which PARP1 inactivation renders cells susceptible to G_2/M cell-cycle arrest or serum-starvation-induced apoptosis.

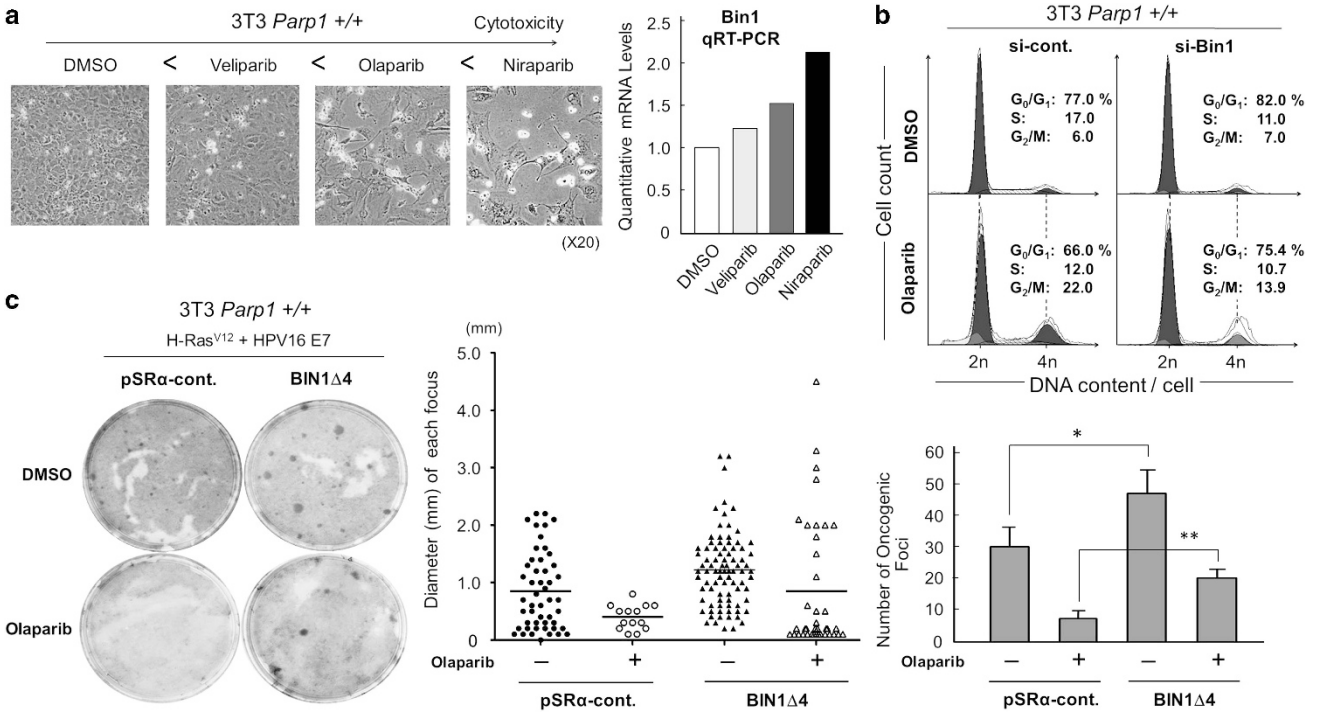

Figure 7 Reduced PARP1-induced BIN1 expression attenuates cancer cell growth. (**a**) Cell morphology of the growing 3T3 *Parp1*$^{+/+}$ fibroblasts in the presence of an indicated PARP inhibitor (5.0 μM, 72 h) (*Left*). qRT-PCR analysis of Bin1 mRNA expression in mouse 3T3 *Parp1*$^{+/+}$ fibroblasts treated with an indicated PARP inhibitor (10 μM, 72 h) (*Right*). (**b**) Cell-cycle profiles of the 3T3 *Parp1*$^{+/+}$ fibroblasts co-transfected with si-control RNA (si-Cont.) or Bin1 si-RNA (si-Bin1) in the presence or absence of olaparib (10 μM) for 72 h. (**c**) Oncogenic foci-formation assay. Mouse 3T3 fibroblasts in a 6-cm dish were transiently co-transfected with two oncogenes, activated *H-Ras* (0.5 μg) and the high-risk human papillomavirus type-16 E7 (*HPV16 E7*) (0.5 μg), with the BIN1 dominant-negative inhibitor–expression vector, pSRα-BIN1Δ4 (1.0 μg), and cultured for 2–3 weeks. The pSRα control vector (1.0 μg) was used as the negative control (*Left*). The diameters of all visible foci were gauged and diagrammed. A horizontal bar shows the average diameter in each transfection group (*Center*). The numbers of all visible foci were scored in each cultured dish (*Right*). The foci-formation assays described here were repeated independently at least three times, and the data were presented as means $\pm$ S.E. *$P<0.05$, **$P<0.005$

Discussion

In this study, we have shown that E2F1 is poly(ADP-ribosyl)ated and interacts with the BIN1 tumor suppressor under normal conditions. Consequently, BIN1 acts as a newly identified E2F1 corepressor, independently of RB1, but only in the presence of PARP1. Because E2F1 activates the *BIN1* gene promoter,[14] the BIN1–E2F1 interaction forms a negative-feedback loop, which may act as a fail-safe device to restrict deregulated E2F1 activity in the absence of RB1. In contrast, when PARP1 is deficient (in response to pharmacological inhibitors or serum starvation), the E2F1 negative-feedback loop is abolished. Therefore, E2F1 is continuously activated and induces E2F1 effector genes, including *BIN1* itself, particularly when RB1 is defective. When the poly(ADP-ribosyl)ation of E2F1 is massively reduced after PARP1 inhibition or serum starvation, BIN1 does not interact with E2F1 and therefore does not suppress the expression of the *BIN1* gene. Consequently, hypo-poly(ADP-ribosyl)ated E2F1 infinitely induces the expression of BIN1, which induces G_2/M arrest in the cell cycle and simultaneously sensitizes cells to E2F1-induced apoptosis during serum starvation (Figure 8).

In addition to the positive role of hypo-poly(ADP-ribosyl)ated E2F1 in E2F1-induced apoptosis during serum deprivation, this study identified a missing link between E2F1-induced gene transcription and cell-cycle progression. Because E2F1 is a major immediate-early transcription factor, E2F1-induced gene expression was thought to be sufficient to promote the G_1/S transition in the cell cycle under normal culture conditions.[5–7] However, we found that E2F1 transactivation is not sufficient to mediate proper cell-cycle progression if the PARP1-dependent G_2/M transition is impaired. Because PARP1 inactivation continuously stimulates endogenous BIN1 expression, which then counteracts the PARP1-dependent G_2/M transition in the cell cycle or mediates E2F1-induced apoptosis after serum withdrawal, the interplay between BIN1 and PARP1 could be a key determinant of E2F1-associated cellular functions, especially when RB1 is dysfunctional. We undertook this study to identify an RB1-deficient mechanism that inhibits the induction of apoptosis by E2F1 during serum starvation, but simultaneously allows E2F1 to promote the cell cycle. Because PARP1 is always abundant in cancer cells, we propose that the reduction of BIN1 levels in cancer cells is a mechanism by which RB1-deficient cancer cells avoid G_2/M cell-cycle arrest, but instead acquire resistance to serum-starvation-induced apoptosis.

A potential and long-standing dilemma associated with the study of tumor suppressors as possible targets for anticancer drugs is that their genes are frequently mutated or deleted in cancer cells. Therefore, it would be impractical or impossible to pharmacologically reactivate a mutated or deleted tumor-suppressor gene in cancer tissues. Unlike many conventional tumor-suppressor genes, the *BIN1* 'tumor-suppressor' gene is

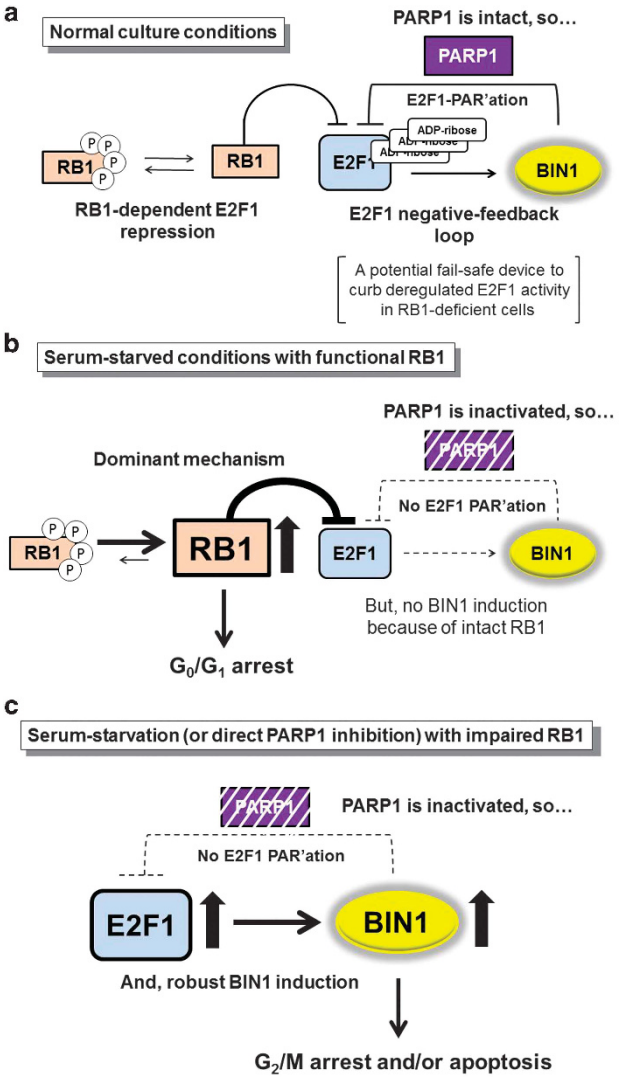

Figure 8 Serum starvation (or PARP1 inactivation) abolishes the E2F1 negative-feedback loop and releases abundant BIN1 proteins in the absence of RB1. (**a**) Under normal culture conditions, endogenous PARP1 is intact, and only small amount of nuclear BIN1 is maintained. The *BIN1* gene is a transcriptional target of E2F1,[14] whereas nuclear BIN1 acts as an E2F1 corepressor. Reduced levels of BIN1 thus allow endogenous E2F1 to induce more BIN1 expression, which then gradually represses E2F1 in a negative-feedback loop. The interaction between E2F1 and BIN1 is stabilized by the poly(ADP-ribosyl)ation of E2F1. Therefore, we propose that the E2F1–BIN1 negative-feedback loop depends on the efficient activity of PARP1 and is controlled independently of conventional hypo-phosphorylated RB1-dependent E2F1 repression. Accordingly, the E2F1–BIN1 interaction may act as a fail-safe device to curb deregulated E2F1 activity, particularly when the RB1-dependent mechanism is deficient. P: phosphorylated. PAR'ation: poly(ADP-ribosyl)ation. (**b**) Although serum starvation massively reduces endogenous E2F1 PAR'ation, it is obvious that the primary biological outcome during serum starvation is not E2F1-induced apoptosis, but RB1-dependent E2F1 repression, which induces G_0/G_1 cell-cycle arrest.[18] This fact clearly suggests that PARP1-inactivation-dependent E2F1 hypo-PAR'ation and subsequent apoptosis during serum starvation does not occur when RB1 is intact (or if E2F1 is not overexpressed). (**c**) In contrast, if PARP1 is inhibited by serum deprivation or more directly by PARP inhibitors in RB1-deficient cells, E2F1 PAR'ation is considerably reduced. The E2F1–BIN1 interaction in the nucleus is then disrupted, allowing E2F1 to constitutively express more BIN1. Because PARP1 activity is essential for the nuclear localization of BIN1, the increase in E2F1 activity caused by PARP1 inhibition releases more BIN1 protein into the cytoplasm, where it induces G_2/M cell-cycle arrest (in the presence of serum) or RB1-independent apoptosis (after serum deprivation).

infrequently mutated or deleted in human malignancies, whereas, like many other tumor-suppressor genes, *BIN1* transcripts and/or BIN1 protein are often reduced or undetectable in cancer cell lines and cancer tissues.[40–43] These deficits are functionally relevant because the heterologous expression of wild-type BIN1 (or in combination with DNA-damaging chemotherapeutic agents, such as cisplatin) frequently induces cell death in advanced cancer cells.[14,27,29–31,35,36] The germline deletion of the *Bin1* gene in mice also supports the anticancer role of BIN1 *in vivo*.[44–46] Importantly, BIN1 has little or no proapoptotic effect on normal or untransformed cells,[31,36] and the BIN1-associated death of cancer cells is independent of p53.[14,27,36] Therefore, our study provides a logical justification for the systemic activation of the *BIN1* gene with a pharmacological approach, such as a PARP inhibitor (as demonstrated above), to restore cancer-selective cell death with little or no adverse effects on untransformed peripheral tissues or even distant organs.

The physiological and pathological roles of human BIN1 protein have recently been shown to extend far beyond its originally predicted role in cancer suppression.[47] Recent evidence has demonstrated the potential significance of BIN1 expression, or its deficiency, not only in cancer pathogenesis,[40–43] but also in the pathophysiology of Alzheimer's disease, where BIN1 may act as a Tau-associated genetic risk factor.[48,49] Cytoplasmic BIN1 also positively regulates the membrane curvature of cardiomyocytes, thereby facilitating the formation and maintenance of cardiac transverse tubules (T-tubules).[50] Consistent with this, cardiac BIN1 acts as a heart-muscle-protective factor, preventing heart failure.[51,52] Given that PARP1 is functionally involved in the pathogenesis of these devastating diseases, partly because of its vital role in oxidative stress responses and apoptosis the PARP1-inhibition-dependent induction of *BIN1* expression, which results in G_2/M cell-cycle arrest and/or E2F1-induced apoptosis (as reported here), may offer a new theoretical basis from which to understand the pathogenesis of these life-threatening diseases in humans.

Materials and Methods

Cell lines. All mammalian cell lines used in the present study except for the cell lines described below were obtained from the American Type Culture Collection (ATCC, Manassas, VA, USA). The mouse 3T3 *Parp1*$^{+/+}$ and 3T3 *Parp1*$^{-/-}$ fibroblast cell lines were generous gifts from F. Dantzer.[25] The *E2f1*$^{-/-}$ MEFs constitutively expressing human E2F1 fused with the recombinant ER (ER-E2F1) have been described previously.[14] All cell lines were maintained in 5% CO_2 at 37 °C, along with the vendor's instructions.

Antibodies, siRNAs (or shRNAs), and oligonucleotide primers. The primary antibodies, si- and shRNAs, and oligonucleotide primers used in this study are listed in the Supplementary Information, Supplementary Tables 1, 2, and 3, respectively.

Plasmid DNAs. The mammalian expression plasmid vectors for human H-Ras^{G12V} (pT22),[29] human BIN1 (CMV-BIN1) and its deletion mutants,[29–31] human RB1 (pSG5-RB1),[15] and hemagglutinin (HA)-tagged human E2F1 (pRcCMV-HA-E2F1)[14,15] have been described previously. The high-risk human papillomavirus type-16 E7-expression vector (p858) was a gift from K. Münger.[53] A luciferase reporter construct driven by the adenoviral *E2A* gene promoter (E2A–Luc),[14,15] the human dihydrofolate reductase gene promoter-driven luciferase vector (DHFR–Luc) (a gift from M. Weitzman), and/or the human c-*myc* gene promoter-driven luciferase vector (c-myc–Luc)[15] were used for the E2F transactivation assays. A luciferase

reporter driven by the human *BIN1* gene promoter (0.8 kb) (BIN1–Luc)[14,15,27,54] was used to monitor the human *BIN1* promoter activity. X-tremeGENE DNA and siRNA reagents (Roche Applied Science, Indianapolis, IN, USA) were used for the transfection of plasmid DNA and siRNA, respectively, according to the vendor's protocols.

Gene-silencing lentivirus production. The pLKO.1-puro (puromycin resistant) lentiviral plasmid vector that expresses shRNAs for human PARP1 (Sigma-Aldrich, St. Louis, MO, USA) was cotransfected into the HEK 293T packaging cell line with the psPAX2 lentivirus packaging vector (Addgene, Cambridge, MA, USA) and the pMD2.G lentivirus VSV-G envelope-expressing vector (Addgene). The pLKO.1-puro vector that expressed scrambled shRNAs was used as the negative control (sh-control). The pcDNA3 vector was transfected instead of the sh-control vector for the mock transfection. The culture medium was collected ~ 72 h post transfection and was centrifuged twice at 670 × *g* for 20 min at room temperature (r.t.) to produce a clear supernatant, which was then overlaid onto a host cell line in the presence of puromycin. All drug-resistant colonies were pooled and cultured for further analysis.

Glutathione *S*-transferase pull-down assays. Glutathione-*S*-transferase (GST) pull-down assays were carried out as described previously.[29] In brief, GST (1.5 μg) or the GST-fusion E2F1 protein (1.5 μg) conjugated with Glutathione Sepharose 4B resin (GE Healthcare Life Sciences, Piscataway, NJ, USA) was incubated with [^{35}S]-methionine-labeled *in vitro*-translated (IVT) proteins at 4 °C for 4 h. The [^{35}S]-labeled IVTs were generated by the T7-TnT Coupled Reticulocyte Lysate System (Promega, Madison, WI, USA). The GST-IVT protein complexes with Sepharose beads were washed three times at 4 °C, subjected to sodium dodecyl sulfate polyacrylamide gel electrophoresis (SDS-PAGE) and fluorographed.

Immunoprecipitation and western blot analysis. Approximately 1.5 mg of pre-cleared protein lysates were incubated with 1.5 μg of an immunoprecipitation (IP) antibody at 4 °C for 4 h with gentle rocking. Purified preimmune IgG (Pierce, Rockford, IL, USA) was used as the negative control. The immunoprecipitated complex was subjected to SDS-PAGE and analyzed by western blotting with a primary antibody. β-Actin was used as the internal loading control. The antibodies used for IP and western blotting are listed in the Supplementary Information, Supplementary Table 1.

Luciferase reporter assay. Luciferase reporter assays were carried out as described previously.[14,15,27,54] To normalize the transfection efficiency, a β-galactosidase expression vector (CMV-β-Gal) was co-transfected with a one-tenth quantity of a luciferase reporter vector.

Real-time PCR and quantitative RT-PCR analysis. One microgram of total RNA was used for first-strand cDNA synthesis using the iScript cDNA Synthesis Kit (Bio-Rad, Hercules, CA, USA). RT-PCRs were performed in 50-μl final volumes, which contained 1 U of Taq DNA polymerase (New England Biolabs, Ipswich, MA, USA), a set of specific primers (0.4 μM each), 2 mM $MgCl_2$, 100 μM dNTPs, and 2 μl of synthesized cDNA. qRT-PCR assays were performed using iQ SYBR Green Supermix (Bio-Rad) in 20-μl reactions containing a set of specific primers (0.2 μM each) and 1 μl of cDNA. The nucleotide sequences of the primers used for RT-PCR/qRT-PCR are listed in the Supplementary Information, Supplementary Table 3.

Chromatin immunoprecipitation assay. ChIP assays were performed as described previously.[14,15,27] The –86/–04 region of the adenoviral *E2A* gene promoter[26] and the –320/–158 region of the human *BIN1* gene promoter[14] were amplified by PCR using 35 cycles at 94 °C for 30 s, 55 °C for 30 s, and 72 °C for 30 s. PCR products were resolved on a 2% agarose gel. The oligonucleotide primers used for the ChIP-PCR are given in the Supplementary Information, Supplementary Table 3.

***In situ* immunofluorescence microscopic analysis.** The cells were fixed in 3.7% formaldehyde, permeabilized with 0.25% Triton X-100 in phosphate-buffered saline (PBS), and soaked in 3% bovine serum albumin (BSA) for blocking at r.t. for 1 h. The anti-BIN1 monoclonal antibody (clone D3), diluted at 1 : 250, was applied to the cells at r.t. for 1 h. The cells were hybridized with mouse-specific secondary antibodies coupled to Alexa Fluor 488 (Molecular Probes, Eugene, OR, USA) diluted 1 : 1000 in blocking buffer, and incubated for 1 h at r.t. in the dark. We used 4′,6-diamidino-2-phenylindole (DAPI) (Sigma-Aldrich, St. Louis, MO, USA) for nuclear counterstaining. The cells were then examined with a Leica DM 5500 fluorescence microscope (Leica Microsystems, Buffalo Grove, IL, USA). The images were recorded with a digital camera, CoolSNAP HQ^2 (Photometrics, Tucson, AZ, USA), attached to the microscope and processed with the imaging software, Leica Application Suite Advanced Fluorescence (Leica Microsystems).

Oncogenic foci formation assay. Mouse 3T3 fibroblasts (0.5×10^5 cells) in a 6-cm tissue-culture dish were transfected with 0.5 μg of the pT22 plasmid DNA (which encodes the human H-Ras^{G12V} oncoprotein[29]) and 0.5 μg of the p858 plasmid vector (which expresses the high-risk HPV16 E7 viral protein[15,53]) in combination with 1.0 μg of the pSRα control vector or 1.0 μg of the pSRα-BIN1Δ4 expression vector.[35] Approximately 72 h post transfection, cells were entirely transferred to a 10-cm dish. Twenty-four hours later, olaparib (AZD2281 or KU-0059436) was added to a final concentration of 5.0 μM.[55] As the vehicle control, 1.0% (v/v) dimethyl sulfoxide (DMSO) was used. The cells were fed twice a week with or without olaparib for 2–3 weeks. All foci were fixed with 100% methanol for 2 min and stained with Giemsa for 30 min.

Flow cytometric analysis. Approximately 1×10^6 cells were treated with 100 units (U) of DNase-free RNase-A at r.t. for 20 min, stained in a solution of propidium iodide (10 μg/ml final concentration) at 4 °C, and sorted by a BD FACSCanto system (BD Biosciences, Franklin Lakes, NJ, USA). We employed the ModFit LT V4 0.5 software (Verity Software House, Topsham, ME, USA) for data analysis in the Flow Cytometry core facility at the GRU Cancer Center (Augusta, GA, USA).

Trypan blue exclusion assay. Trypsinized cells were suspended in PBS at r.t., then 20 μl of this cell suspension was mixed with 20 μl of trypan blue solution (HyClone, Logan, UT, USA), and 10 μl of this mixture was used for counting blue (dead) and white (alive) cells using a hemocytometer.

Statistical analysis. All cell-based assays described in this study were repeated independently at least three times. The data were analyzed with Microsoft Excel (Microsoft Co., Redmond, WA, USA) and are presented as mean ± S.E. Statistical significance was determined with Student's *t*-test, and *P*-values less than 0.05 (**P*), 0.005 (***P*), or 0.0005 (****P*) were considered statistically significant.

Conflict of Interest

DS holds a 1999 US Patent with GC Prendergast, no. 6,410,238, 'Box-dependent Myc-interacting protein (Bin1) compositions and uses thereof' (The Wistar Institute of Anatomy and Biology, Philadelphia, PA, USA).

Acknowledgements. We thank F Dantzer, M Weitzman, and K Münger for the reagents; W King for technical assistance with flow cytometry; GC Prendergast for helpful discussion; and M Herlyn for critical reading of the manuscript. This work was supported in part by grants from the US National Institutes of Health (NIH) (R01CA140379) and the US Army Department of Defense Prostate Cancer Research Program (DAMD 17-02-1-0131) (to DS). TI was the recipient of the 2013-2014 Kobe University Presidential Award for International Education and Research. EKC was the recipient of the Ruth L. Kirschstein National Research Service Award for Predoctoral Training (NIH F31).

Author contributions

A.K., T.I., S.P., E.K.C., C.D.P., and D.S. performed the experiments and analyzed the data; D.S. designed the experiments, supervised the project, and wrote the manuscript.

1. Guo XE, Ngo B, Modrek AS, Lee WH. Targeting tumor suppressor networks for cancer therapeutics. *Curr Drug Targets* 2014; **15**: 2–16.
2. Orr B, Compton DA. A double-edged sword: how oncogenes and tumor suppressor genes can contribute to chromosomal instability. *Front Oncol* 2013; **3**: 164.
3. Hanel W, Moll UM. Links between mutant p53 and genomic instability. *J Cell Biochem* 2012; **113**: 433–439.
4. Moody CA, Laimins LA. Human papillomavirus oncoproteins: pathways to transformation. *Nat Rev Cancer* 2010; **10**: 550–560.

5. Polager S, Ginsberg D. p53 and E2f: partners in life and death. *Nat Rev Cancer* 2009; **9**: 738–748.
6. Johnson DG, Degregori J. Putting the oncogenic and tumor suppressive activities of E2F into context. *Curr Mol Med* 2006; **6**: 731–738.
7. Stanelle J, Pützer BM. E2F1-induced apoptosis: turning killers into therapeutics. *Trends Mol Med* 2006; **12**: 177–185.
8. Moroni MC, Hickman ES, Lazzerini Denchi E, Caprara G, Colli E, Cecconi F *et al.* Apaf-1 is a transcriptional target for E2F and p53. *Nat Cell Biol* 2001; **3**: 552–558.
9. Furukawa Y, Nishimura N, Furukawa Y, Satoh M, Endo H, Iwase S *et al.* Apaf-1 is a mediator of E2F-1-induced apoptosis. *J Biol Chem* 2002; **277**: 39760–39768.
10. Nahle Z, Polakoff J, Davuluri RV, McCurrach ME, Jacobson MD, Narita M *et al.* Direct coupling of the cell cycle and cell death machinery by E2F. *Nat Cell Biol* 2002; **4**: 859–864.
11. Komori H, Enomoto M, Nakamura M, Iwanaga R, Ohtani K. Distinct E2F-mediated transcriptional program regulates p14ARF gene expression. *EMBO J* 2005; **24**: 3724–3736.
12. del Arroyo AG, El Messaoudi S, Clark PA, James M, Stott F, Bracken A *et al.* E2F-dependent induction of p14ARF during cell cycle re-entry in human T cells. *Cell Cycle* 2007; **6**: 2697–2705.
13. Stiewe T, Pützer BM. Role of the p53-homologue p73 in E2F1-induced apoptosis. *Nat Genet* 2000; **26**: 464–469.
14. Cassimere EK, Pyndiah S, Sakamuro D. The c-MYC-interacting proapoptotic tumor suppressor BIN1 is a transcriptional target for E2F1 in response to DNA damage. *Cell Death Differ* 2009; **16**: 1641–1653.
15. Kinney EL, Tanida S, Rodrigue AA, Johnson JK, Tompkins VS, Sakamuro D. Adenovirus E1A oncoprotein liberates c-Myc activity to promote cell proliferation through abating Bin1 expression *via* an Rb/E2F1-dependent mechanism. *J Cell Physiol* 2008; **216**: 621–631.
16. Yamasaki L, Jacks T, Bronson R, Goillot E, Harlow E, Dyson NJ. Tumor induction and tissue atrophy in mice lacking E2F-1. *Cell* 1996; **85**: 537–548.
17. Field SJ, Tsai FY, Kuo F, Zubiaga AM, Kaelin Jr WG, Livingston DM *et al.* E2F-1 functions in mice to promote apoptosis and suppress proliferation. *Cell* 1996; **85**: 549–561.
18. Dick FA, Rubin SM. Molecular mechanisms underlying RB protein function. *Nat Rev Mol Cell Biol* 2013; **14**: 297–306.
19. Di Fiore R, D'Anneo A, Tesoriere G, Vento R. RB1 in cancer: different mechanisms of RB1 inactivation and alterations of pRb pathway in tumorigenesis. *J Cell Physiol* 2013; **228**: 1676–1687.
20. Gibson BA, Kraus WL. New insights into the molecular and cellular functions of poly(ADP-ribose) and PARPs. *Nat Rev Mol Cell Biol* 2012; **13**: 411–424.
21. Luo X, Kraus WL. On PAR with PARP: cellular stress signaling through poly(ADP-ribose) and PARP-1. *Gene Dev* 2012; **26**: 417–432.
22. Ji Y, Tulin AV. The roles of PARP1 in gene control and cell differentiation. *Curr Opin Genet Dev* 2010; **20**: 512–518.
23. Kummar S, Chen A, Parchment RE, Kinders RJ, Ji J, Tomaszewski JE *et al.* Advances in using PARP inhibitors to treat cancer. *BMC Med* 2012; **10**: 25.
24. Simbulan-Rosenthal CM, Rosenthal DS, Luo R, Samara R, Espinoza LA, Hassa PO *et al.* PARP-1 binds E2F-1 independently of its DNA binding and catalytic domains, and acts as a novel coactivator of E2F-1-mediated transcription during re-entry of quiescent cells into S phase. *Oncogene* 2003; **22**: 8460–8471.
25. Dantzer F, de La Rubia G, Ménissier-De Murcia J, Hostomsky Z, de Murcia G, Schreiber V. Base excision repair is impaired in mammalian cells lacking Poly(ADP-ribose) polymerase-1. *Biochemistry* 2000; **39**: 7559–7569.
26. Kovesdi I, Reichel R, Nevins JR. Role of an adenovirus E2 promoter binding factor in E1A-mediated coordinate gene control. *Proc Natl Acad Sci USA* 1987; **84**: 2180–2184.
27. Pyndiah S, Tanida S, Ahmed KM, Cassimere EK, Choe C, Sakamuro D. c-MYC suppresses BIN1 to release poly(ADP-ribose) polymerase 1: a mechanism by which cancer cells acquire cisplatin resistance. *Sci Signal* 2011; **4**: ra19.
28. Chiou SH, Jiang BH, Yu YL, Chou SJ, Tsai PH, Chang WC *et al.* Poly(ADP-ribose) polymerase 1 regulates nuclear reprogramming and promotes iPSC generation without c-Myc. *J Exp Med.* 2013; **210**: 85–98.
29. Sakamuro D, Elliott KJ, Wechsler-Reya R, Prendergast GC. BIN1 is a novel MYC-interacting protein with features of a tumour suppressor. *Nat Genet* 1996; **14**: 69–77.
30. Elliott K, Sakamuro D, Basu A, Du W, Wunner W, Staller P *et al.* Bin1 functionally interacts with Myc and inhibits cell proliferation *via* multiple mechanisms. *Oncogene* 1999; **18**: 3564–3573.
31. Lundgaard GL, Daniels NE, Pyndiah S, Cassimere EK, Ahmed KM, Rodrigue A *et al.* Identification of a novel effector domain of BIN1 for cancer suppression. *J Cell Biochem* 2011; **112**: 2992–3001.
32. Yelamos J, Farres J, Llacuna L, Ampurdanes C, Martin-Caballero J. PARP-1 and PARP-2: New players in tumour development. *Am J Cancer Res* 2011; **1**: 328–346.
33. Szántó M, Brunyánszki A, Kiss B, Nagy L, Gergely P, Virág L *et al.* Poly(ADP-ribose) polymerase-2: emerging transcriptional roles of a DNA-repair protein. *Cell Mol Life Sci* **69**: 4079–40922012.
34. Murai J, Huang SY, Das BB, Renaud A, Zhang Y, Doroshow JH *et al.* Trapping of PARP1 and PARP2 by clinical PARP inhibitors. *Cancer Res* 2012; **72**: 5588–5599.
35. DuHadaway JB, Sakamuro D, Ewert DL, Prendergast GC. Bin1 mediates apoptosis by c-Myc in transformed primary cells. *Cancer Res* 2001; **61**: 3151–3156.
36. Elliott K, Ge K, Du W, Prendergast GC. The c-Myc-interacting adaptor protein Bin1 activates a caspase-independent cell death program. *Oncogene* 2000; **19**: 4669–4684.
37. Casal E, Federici L, Zhang W, Fernandez-Recio J, Priego EM, Miguel RN *et al.* The crystal structure of the BAR domain from human Bin1/amphiphysin II and its implications for molecular recognition. *Biochemistry* 2006; **45**: 12917–12928.
38. Arnold K, Bordoli L, Kopp J, Schwede T. The SWISS-MODEL Workspace: A web-based environment for protein structure homology modelling. *Bioinformatics* 2006; **22**: 195–201.
39. Kelley LA, Sternberg MJE. Protein structure prediction on the web: a case study using the Phyre server. *Nat Protocol* 2009; **4**: 363–371.
40. Ge K, DuHadaway J, Du W, Herlyn M, Rodeck U, Prendergast GC. Mechanism for elimination of a tumor suppressor: aberrant splicing of a brain-specific exon causes loss of function of Bin1 in melanoma. *Proc Natl Acad Sci USA* 1999; **96**: 9689–9694.
41. Ge K, Duhadaway J, Sakamuro D, Wechsler-Reya R, Reynolds C, Prendergast GC. Losses of the tumor suppressor BIN1 in breast carcinoma are frequent and reflect deficits in programmed cell death capacity. *Int J Cancer* 2000; **85**: 376–383.
42. Ge K, Minhas F, Duhadaway J, Mao N-C, Wilson D, Buccafusca R *et al.* Loss of heterozygosity and tumor suppressor activity of Bin1 in prostate carcinoma. *Int J Cancer* 2000; **86**: 155–161.
43. Ghaneie A, Zemba-Palko V, Itoh H, Itoh K, Sakamuro D, Nakamura S *et al.* Bin1 attenuation in breast cancer is correlated to nodal metastasis and reduced survival. *Cancer Biol Ther* 2007; **6**: 192–194.
44. Chang MY, Boulden J, Sutanto-Ward E, Duhadaway JB, Soler AP, Muller AJ *et al.* Bin1 ablation in mammary gland delays tissue remodeling and drives cancer progression. *Cancer Res* 2007a; **67**: 100–107.
45. Chang MY, Boulden J, Katz B, Wang L, Meyer TJ, Soler AP *et al.* Bin1 ablation increases susceptibility to cancer during aging, particularly lung cancer. *Cancer Res* 2007b; **67**: 7605–7612.
46. Prendergast GC, Muller AJ, Ramalingam A, Chang MY. BAR the door: cancer suppression by amphiphysin-like genes. *Biochim Biophys Acta* 2009; **1795**: 25–36.
47. Prokic I, Cowling BS, Laporte J. Amphiphysin 2 (BIN1) in physiology and diseases. *J Mol Med (Berl)* 2014; **92**: 453–463.
48. Kingwell K. Alzheimer disease: BIN1 variant increases risk of Alzheimer disease through tau. *Nat Rev Neurol* 2013; **9**: 184.
49. Tan MS, Yu JT, Tan L. Bridging integrator 1 (BIN1): form, function, and Alzheimer's disease. *Trends Mol Med* 2013; **19**: 594–603.
50. Hong T, Yang H, Zhang SS, Cho HC, Kalashnikova M, Sun B *et al.* Cardiac BIN1 folds T-tubule membrane, controlling ion flux and limiting arrhythmia. *Nat Med* 2014; **20**: 624–632.
51. Hong TT, Smyth JW, Chu KY, Vogan JM, Fong TS, Jensen BC *et al.* BIN1 is reduced and Cav1.2 trafficking is impaired in human failing cardiomyocytes. *Heart Rhythm* 2012; **9**: 812–820.
52. Hong TT, Cogswell R, James CA, Kang G, Pullinger CR, Malloy MJ *et al.* Plasma BIN1 correlates with heart failure and predicts arrhythmia in patients with arrhythmogenic right ventricular cardiomyopathy. *Heart Rhythm* 2012; **9**: 961–967.
53. Münger K, Yee CL, Phelps WC, Pietenpol JA, Moses HL, Howley PM. Biochemical and biological differences between E7 oncoproteins of the high- and low-risk human papillomavirus types are determined by amino-terminal sequences. *J Virol* 1991; **65**: 3943–3948.
54. Wechsler-Reya RJ, Sakamuro D, Zhang J, Duhadaway J, Prendergast GC. Structural analysis of the human *BIN1* gene. Evidence for tissue-specific transcriptional regulation and alternate RNA splicing. *J Biol Chem* 1997; **272**: 31453–31458.
55. Menear KA, Adcock C, Boulter R, Cockcroft XL, Copsey L, Cranston A *et al.* 4-[3-(4-cyclopropanecarbonylpiperazine-1-carbonyl)-4-fluorobenzyl]-2H-phthalazin-1-one: a novel bioavailable inhibitor of poly(ADP-ribose) polymerase-1. *J Med Chem* 2008; **51**: 6581–6591.

Supplementary Information accompanies this paper on Cell Death and Differentiation website (http://www.nature.com/cdd)